The energy dependence of the conductance and scattering wave functions of a 2D quantum dot

1995 J. Phys.: Condens. Matter 7 6717

(http://iopscience.iop.org/0953-8984/7/33/010)

J. Phys.: Condens. Matter 7 (1995) 6717–6726. Printed in the UK

The energy dependence of the conductance and scattering wave functions of a 2D quantum dot

P N Butcher† and J A McInnes‡

† Department of Physics, University of Warwick, Coventry CV4 7AL, UK
‡ Department of Computer Science, University of Strathclyde, Glasgow G1 1XH, UK

Received 18 April 1995, in final form 27 June 1995

Abstract. A new wave-function matching formalism is used to calculate wave functions ψ and the conductance g_{12} for a quantum dot as functions of the Fermi wavelength λ. The dot is formed in a 2D quantum wire with hard walls by pushing in through one wall two identical, hard-wall, rectangular fingers with height h, width d and separation s. Calculations of conductance g_{12} are made for a structure which exhibits two resonant tunnelling peaks below the nominal transmission threshold over the tops of the fingers. These peaks are associated with the open-ended organ pipe modes in the region between the fingers. The two longest organ pipe resonant wavelengths are within 2% and 10% of the calculated peak positions, but wave-function spillage over the tops of the fingers and the space between them has a marked effect on both the resonant wave functions and the resonant wavelengths. Contour plots of $|\psi|^2$ for scattering waves are presented and used to elucidate the behaviour of g_{12}.

1. Introduction

In a recent paper [1], hereafter referred to as I, the authors describe a widely applicable new procedure for calculating conductances and scattering wave functions for 2D hard-wall nanostructures. To test the procedure, calculations are reported in I for a ballistic 2D quantum wire with one hard-wall finger pushed in through one side. In this paper, we use the same procedure to calculate conductances and scattering wave functions when *two* hard wall fingers are pushed in through one side to form a quantum dot. Studies of wave functions in other structures using different matching procedures are reported in references [2–14].

We suppose that the 2DEG is at absolute zero and is spin degenerate with a Fermi wavelength denoted by λ. The conductance g_{12} is calculated in units of $2e^2/h$ as a function of $2w/\lambda$ where w is the width of the quantum wire. Our main concern is the resonant tunnelling peaks which arise when $2w/\lambda$ is below the nominal propagation threshold of the structure and is close to a resonant value for one of the open-ended organ pipe resonances of the quantum dot. We calculate the behaviour of the resonant peaks as the finger height h and width d are varied and give contour plots of $|\psi|^2$ (where ψ is a scattering wave function) in the neighbourhood of the resonances.

The plan of the paper is as follows. In section 2 we describe the nanostructure and introduce some relevant notation. Section 3 is devoted to the dependence of g_{12} on $2w/\lambda$. In section 4 we study the behaviour of the contour plots of $|\psi|^2$, and in section 5 we draw some conclusions.

0953-8984/95/336717+10$19.50

2. The nanostructure and the method of calculation

The nanostructure is shown schematically in figure 1. Terminals 1 and 2 are assumed to be ideal electron waveguides which inject electrons into the region between the vertical dashed lines, which we refer to as 'interfaces'. The full lines are hard walls at which the electronic potential energy rises to infinity. Inside these walls, the potential energy is set equal to zero. The notation used for the various dimensions of the nanostructure is indicated in the figure. The fingers are identical with height h, width d and spacing s. The height above the fingers is denoted by $w' = w - h$ where w is the width of the quantum wire. The region between the interfaces is referred to as the 'cavity'.

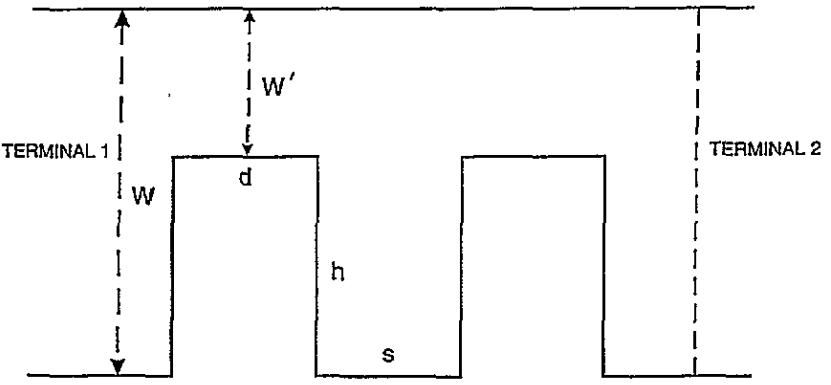

Figure 1. A sketch of the nanostructure giving the notation used for its dimensions. The full lines are hard potential walls.

The calculations are carried out by computing a set of cavity functions, each one of which matches a quantum wire mode in magnitude and sign across one interface, and vanishes on the other interface. We can then set up a general wavefunction for the entire structure which is *continuous* everywhere by taking an arbitrary superposition of cavity wave functions, each one of which is extended continuously into both terminals. We relate these coefficients of the modes in this general wave function by performing a least squares minimization of the total error in the continuity of the normal derivative of ψ across both interfaces. We are then in a position to determine the scattering matrix, the conductance g_{12} between terminals 1 and 2, and the wave function for any given set of quantum wire modes incident on the structure. All the propagating modes in the quantum wires are included in the calculation and the number of evanescent modes is increased until satisfactory convergence is achieved for g_{12} and the wave functions. Full details are given in I.

3. The dependence of the conductance on the Fermi wavelength

We consider first a structure in which the fingers have height $h = 0.7w$ and width $d = 0.4w$. The dashed curve in figure 2 shows g_{12} in units of $2e^2/h$ when only one finger is present (this structure is considered in detail in I). To a reasonably good approximation, g_{12} is equal to the number of modes which can propagate in the region *above* the finger. Let us write $w' = w - h = 0.3w$ for the width of this region. Then, the number of propagating modes above the finger is the largest integer in $2w'/\lambda = (w'/w)\ 2w/\lambda = 0.3 \times 2w/\lambda$.

Consequently, $g_{12} \to 0$ when $2w/\lambda$ falls below $w/w' = 3.33$, and increases to the integer n when $2w/\lambda$ goes through $n/0.3 = 3.33n$. We refer to w/w' as the 'nominal threshold' value of $2w/\lambda$ in what follows. The dashed curve in figure 2 exhibits the above behaviour, but also has small oscillations at the beginning of each conductance plateau. The oscillations are due to weak reflection of the waves propagating above the finger at the sharp corners of the finger [1, 3]. The full line in figure 2 shows g_{12} calculated for two fingers spaced by an arbitrarily chosen value of $s = 0.467w$. We see that g_{12} apparently continues to vanish below the nominal threshold (but see below for a correction to this observation). Above the nominal threshold, g_{12} shows strong oscillations because there are strong multiple reflections in the region between the two fingers. The heights of the peaks increase as new modes begin to propagate above the fingers, but never exceed g_{12} for one finger.

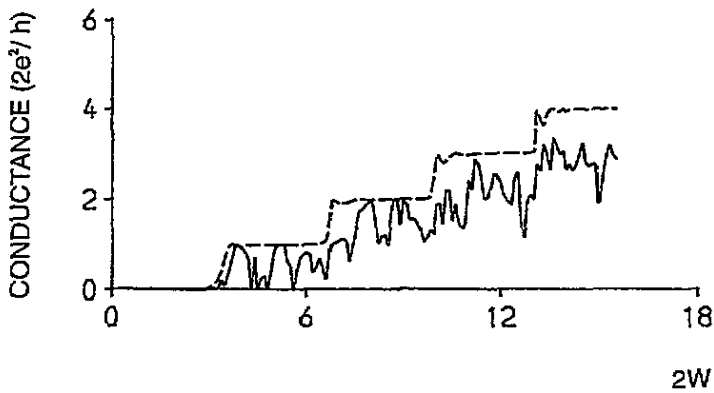

Figure 2. A plot of conductance above the nominal threshold against $2w/\lambda$ when $d/w = 0.4$, $h/w = 0.7$, $s/w = 0.467$ and $w'/w = 0.3$. The full curve is calculated for the structure shown in figure 1. The dashed curve is for the case when one finger is removed.

It was expected that resonant tunnelling peaks would be found below the nominal threshold. Their absence from figure 2 is due to the relatively large value of finger thickness, $d = 0.3w$, used in the calculations which is in the same order as most of the values of d used in I. The width of the resonant tunnelling peaks is a strong function of d. When $d = 0.3w$ the peaks exist, but are so narrow that calculations for very small incremental steps of $2w/\lambda$ failed to reveal them in figure 2. In figure 3 we plot g_{12} against $2w/\lambda$ below the nominal threshold when d is reduced to $0.1w$ and the remaining dimensions are the same as those used in figure 2. We now find two resonant tunnelling peaks at $2w/\lambda = 2.214$ and 2.743 at which $g_{12} = 1$.

The location of the peaks is close to the two lowest resonant $2w/\lambda$ values for the open-ended space between the fingers. We write the resonant values of λ in this space in the form λ_{mn} where m is a positive integer and n is a positive odd integer. Then

$$\frac{2w}{\lambda_{mn}} = \left(\left[\frac{mw}{s}\right]^2 + \left[\frac{nw}{2h}\right]^2\right)^{1/2}. \tag{1}$$

The corresponding solutions of the wave equation (in which the potential energy is zero) vanish on the hard walls at the bottom and the sides of the space considered, and has zero

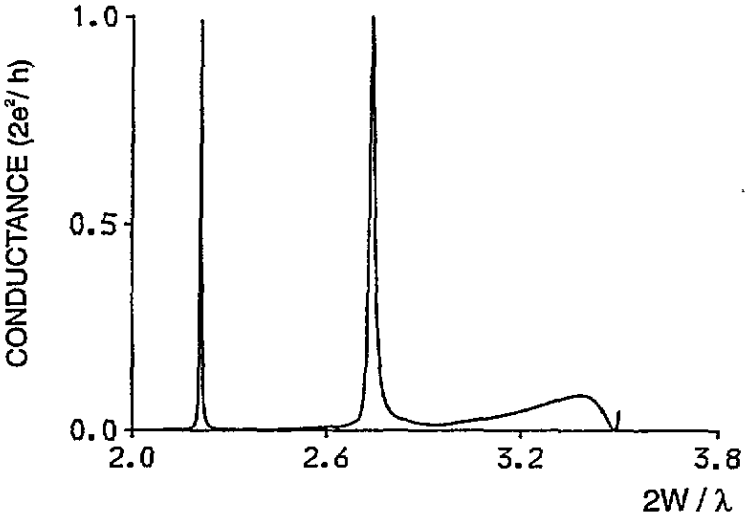

Figure 3. A plot of conductance below the nominal threshold against $2w/\lambda$ when $d/w = 0.1$ and the other dimensions have the values given in figure 2.

normal derivative on a horizontal straight line joining the tops of the fingers. We draw attention to the fact that w cancels out of (1). It is introduced because all other lengths are expressed in terms of it in our calculations. The two lowest values of $2w/\lambda_{mn}$ derived from (1) are $2w/\lambda_{11} = 2.26$ and $2w/\lambda_{13} = 3.03$ which are within 2% and 10% respectively of the values at the resonant peaks in figure 3. The error arises because (1) is a useful but crude approximation. It takes no account of the 'spillage' of the wave functions both above the region between the two fingers, and over the finger tops which we discuss in section 4. All the other open-ended organ pipe resonances are above the nominal threshold and contribute to the oscillatory structure shown in figure 2.

To illustrate the effect of spillage, we plot the resonant peaks in figure 4 for $d = 0.1w$, as in figure 3, and $h/w = 0.667$ (long dashes), 0.700 (long and short dashes), 0.733 (short dashes), 0.767 (medium-sized dashes) and 0.800 (full line). Equation (1) predicts that $2w/\lambda_{11}$ and $2w/\lambda_{13}$ both increase as h is reduced. We see from figure 4 that the opposite happens because decreasing h increases the aperture $w' = w - h$ above the fingers which increases the wave function spillage. In the next section, we present wave-function contours which confirm this explanation. We also see in figure 4 that the width of the resonances increases as h/w is reduced, which is consistent with increased leakage into the region above the fingers. Finally, we see from figure 4 that, for the smallest value of h/w considered; 0.667 (long dashes), the broad second resonance lies on the rising curve of g_{12} which precedes the nominal threshold at $2w/\lambda = 3$. We would also expect spillage to increase when the flat fingers considered up till now are replaced by fingers with the same width ($0.1w$) for which the same overall height h is achieved by shorter fingers (with h reduced by r) capped with semicircles of radius r. Our calculations confirm this expectation and are shown in figure 5. The positions of the resonances move to lower $2w/\lambda$ values as we move from flat-topped fingers (dashed line) to round-topped fingers (solid line). The resonances also broaden due to the increased spillage.

Finally, in figure 6 we revert to flat-topped fingers in order to show the effect on the second resonance of its passage through the nominal threshold. The dotted curve is taken from figure 4 and has $h/w = 0.667$. The second resonance peak is well below the nominal

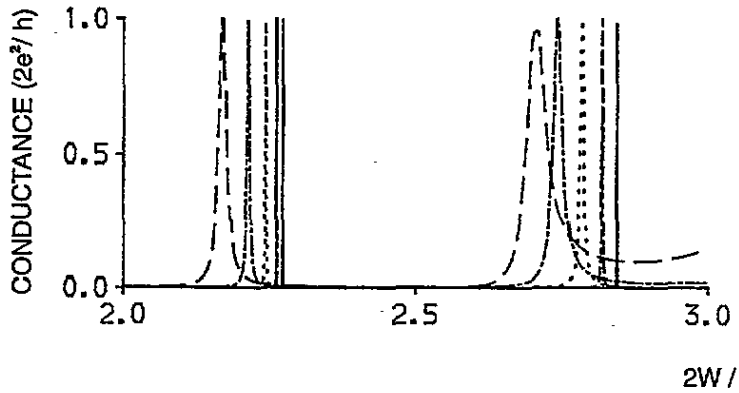

Figure 4. The dependence of the resonance peaks on finger height for high fingers. The curves are drawn for $d/w = 0.1$ and $h/w = 0.8$ (——), 0.767 (— — —), 0.733 (- - - -), 0.700 (chain) and 0.667 (— · —). The other dimensions have the values given in figure 2.

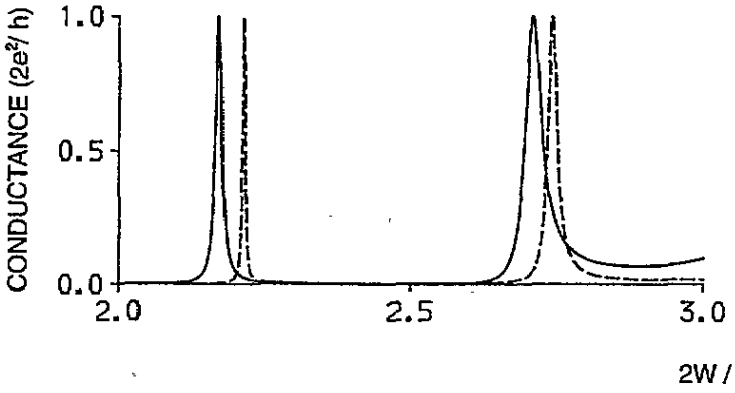

Figure 5. The dependence of the resonance peaks on finger shape for high fingers. The curves are drawn with $d/w = 0.1$ for rounded fingers (full line) and for flat-topped fingers (dashed line). The other dimensions have the values given in figure 2.

threshold at $2w/\lambda = 3$ and consequently suffers very little distortion. The dashed curve has $h/w = 0.6$. The nominal threshold is at $2w/\lambda = 2.5$ and the second resonance is now almost obscured by the beginning of the first region of strong propagation. Finally, the solid curve has $h/w = 0.533$. The nominal threshold is at $2w/\lambda = 2.14$ and a short plateau with $g_{12} = 1$ completely obscures the second resonance. In this case, the first resonance peak has moved to $2w/\lambda = 1.89$ and is followed by a pseudo-plateau with $g_{12} = 0.26$ extending from $2w/\lambda = 2.0$ to 2.4. We notice that, in all three cases, $g_{12} = 0$ near to $2w/\lambda = 2.6$ which is just below the second resonance. When $h/w = 0.533$, this zero delays the onset of a region where $g_{12} \sim 1$ until $2w/\lambda$ is well above the nominal threshold.

4. The behaviour of the wave function near resonance and on plateaux

In this section, we present contour plots of $|\psi|^2$ when the 'dominant' mode is incident in

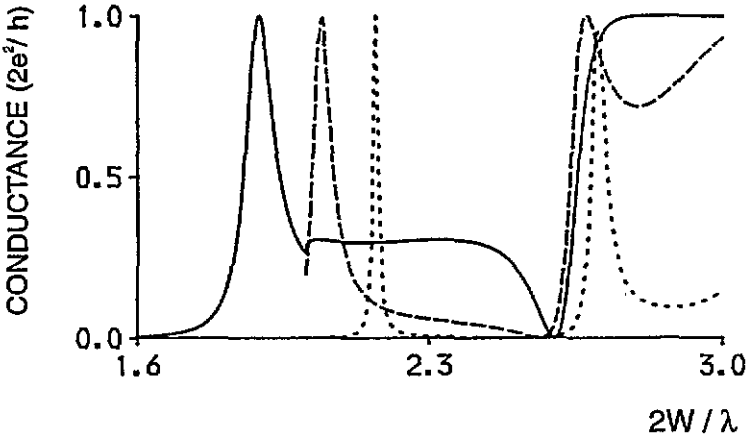

Figure 6. The dependence of the resonance peaks on finger height for low fingers. The curves are drawn for $d/w = 0.1$ and $h/w = 0.667$ (----), 0.6 (— — —) and 0.533 (——) for which the nominal threshold is at $2w/\lambda = 3$, 2.5 and 2.14 respectively. The other dimensions have the values given in figure 2.

terminal 1. (The dominant mode begins to propagate in the terminals when $2w/\lambda = 1$.) Figure 7 shows the contours for the structure described in figure 3 when $2w/\lambda = 2.214$, i.e. at the centre of the first resonance peak. The contours are largely confined in the regions between the fingers but there is considerable 'spillage' above the space between them and over their tops. In both terminals, $|\psi|^2$ is too small to appear on the contour scale used in figure 7. The contours are almost symmetrical about the centre line of the structure (at $x/2w = 0.5$) in spite of the asymmetric excitation. This is because the dominant mode incident in terminal 1 strongly excites the lowest organ-pipe resonance between the fingers which is symmetrical. The contours in figure 8 are drawn for the same structure when $2w/\lambda = 2.35$ (which is just above the first resonance peak in figure 3 with $g_{12} \simeq 0.044$). The contours are all concentrated on the left of the diagram where a strong standing-wave pattern appears in terminal 1 because the dominant mode is almost totally reflected. On the contour scale used in figure 8, no contours appear either between the fingers or in terminal 2. Similar behaviour is found when $2w/\lambda = 2.15$ which is just below the first resonance peak.

In figures 9, 10 and 11, we plot contours of $|\psi|^2$ when h/w is increased from 0.533 to 0.7. The variation of g_{12} in this case is given by the full line in figure 6. The contours in figure 9 are drawn for $2w/\lambda = 1.89$ which is at the centre of the first resonance peak. We see that there is a fairly strong build-up of $|\psi|^2$ over the entire region in the space both between the fingers and above their tops. Moreover, the position of the maximum in $|\psi|^2$ has moved from just inside the space between fingers in figure 7 to just outside it in figure 9. The contours in figure 10 are drawn for $2w/\lambda = 2.2$ which is the middle of the pseudo-plateau where $g_{12} = 0.298$ in figure 6. There is now a strong standing-wave pattern in terminal 1, weak excitation of $|\psi|^2$ in the space between the fingers and, as we would expect, weaker excitation of $|\psi|^2$ in terminal 2. Finally, in figure 11, we show the contours of $|\psi|^2$ when $2w/\lambda = 2.85$, which is on the short plateau with $g_{12} = 1$, which is exhibited by the full curve in figure 6. We see that the incident dominant mode now excite a T-shaped symmetrical resonance in $|\psi|^2$ which is spread over the entire T-shaped region in between and above the fingers. Moreover $|\psi|^2$ has a minimum near the tops of the fingers. Since $h/w = 0.533$ this minimum is close to that exhibited by mode 2 in the

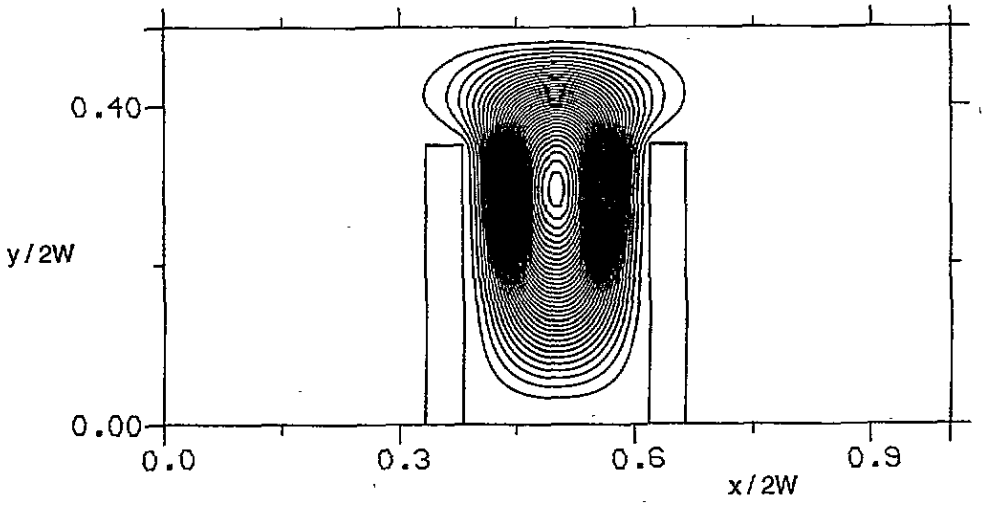

Figure 7. Contours of $|\psi|^2$ for the structure described in figure 3. The contours are drawn for $2w/\lambda = 2.214$ (i.e. the centre of the first resonance peak in figure 3).

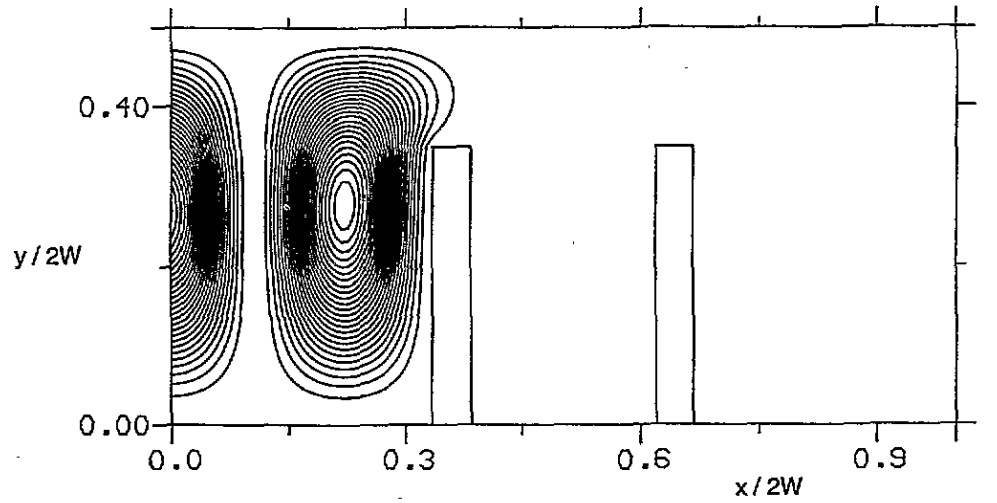

Figure 8. Contours of $|\psi|^2$ for the structure described in figure 3. The contours are drawn for $2w/\lambda = 2.35$ which is just above the first resonance peak in figure 3.

terminals, which begins to propagate when $2w/\lambda > 2$ and has $\psi = 0$ on the centre on the line of the terminals. Consequently, we expect to find mode 2 strongly excited in terminal 2. The pattern of contours shown there in figure 11 indicates that this is the case. The pattern of contours in terminal 1, on the other hand, indicates that mode 1 suffers considerable reflection from the quantum dot.

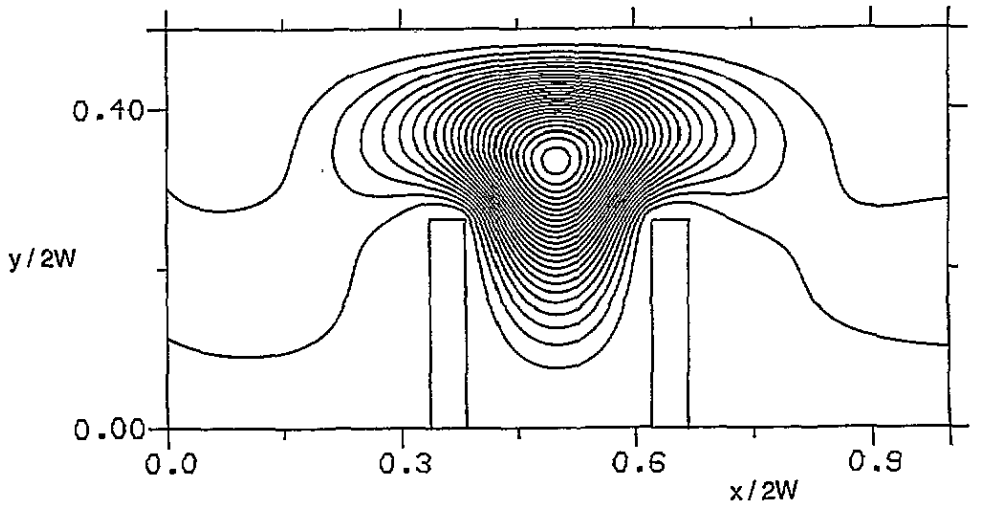

Figure 9. Contours of $|\psi|^2$ for the structure described in figure 6 when $h/w = 0.533$. The contours are drawn for $2w/\lambda = 1.89$ which is at the centre of the first resonance peak.

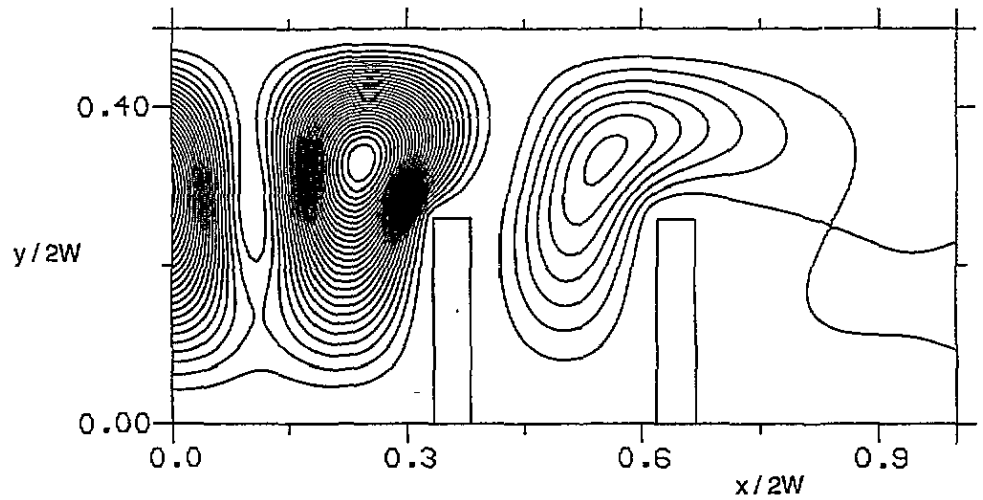

Figure 10. Contours of $|\psi|^2$ for the structure described in figure 6 when $h/w = 0.533$. The contours are drawn for $2w/\lambda = 2.20$ which is near the middle of the pseudo-plateau where $g_{12} = 0.298$.

5. Conclusion

The numerical results presented in the figures show that useful data for g_{12} and $|\psi|^2$ for a quantum dot can be generated by using the numerical procedure described in I. In the interpretation of the data we have, in the interests of brevity, concentrated attention largely on the first resonance peak of g_{12}. The simple model used to predict the location of the resonance peak should not be taken too seriously. It helped us to find the resonant values of $2w/\lambda$ but it totally ignores the effect of wave-function spillage outside the region between

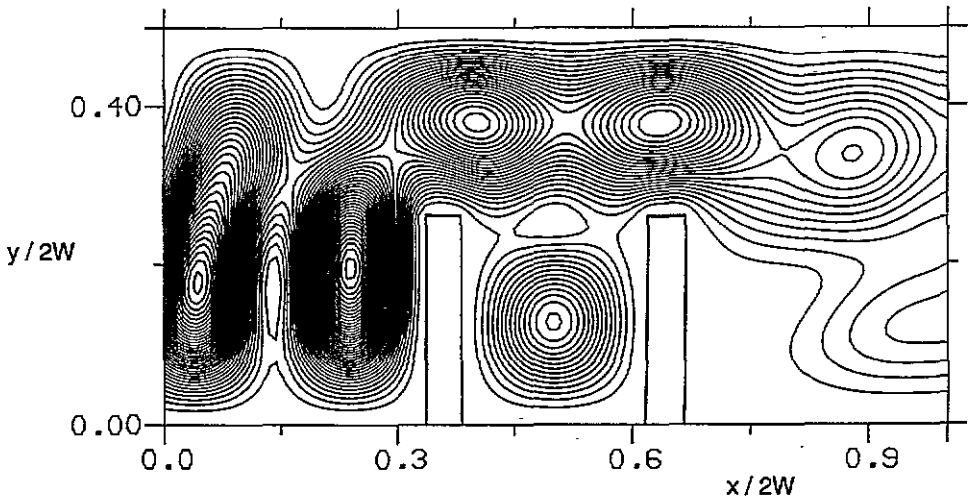

Figure 11. Contours of $|\psi|^2$ for the structure described in figure 6 where $h/w = 0.533$. The contours are drawn for $2w/\lambda = 2.85$ at which $g_{12} = 1$.

the fingers which is always significant. It becomes increasingly important as h/w decreases from 0.7 as in figure 7 to 0.533 as in figure 9. In particular, we have seen that the maximum of $|\psi|^2$ moves from just inside to outside the region between the fingers. This feature is not present in our simple model, which is part of the reason why the model predicts that the first resonant values of $2w/\lambda$ increase as h/w decreases whereas, in reality, they decrease. The other part of the reason is the spreading out of $|\psi|^2$ over both the tops of the fingers and the space between them (which is shown best in figure 9) which is also neglected in the model.

One might consider improving on this behaviour by fitting half-period sine functions between the hard walls in both the x and y directions. Then h is irrelevant and consequently the first resonance value remains constant at $2w/\lambda = 2.36$ instead of moving the wrong way. This result is exact when $h/w = 1$ because the dot is then completely enclosed by hard walls. It stays constant when h/w is reduced because it only allows (approximately) for spillage above the space between the fingers and ignores the spillage over their tops. Both these components of the spillage are important. In our calculation, h/w varies between 0.533 and 0.8. The computed values of $2w/\lambda_{11}$ at the ends of this range are 1.89 and 2.27 respectively. The two approximate formulae yield results for $2w/\lambda_{11}$ which are always close to each other with the open-ended result nearer to the computed value. There is little to be gained by elaboration of these elementary models. Numerical models are essential in quantitative studies of the behaviour of quantum dots.

We have confined our attention here to a strictly 2D electron gas moving in the xy plane. In practice the system to be considered is a 3D electron gas subjected to a confining potential $V(z)$ created by one or more planar heterojunctions. The typical width of $V(z)$ is in the order of 10 nm. To make a structure of the type considered here, split gates are usually used to create a confining potential $V(y)$ in the y direction with a width $\simeq 300$ nm. Consequently, the energy levels ϵ_{zn} (with $n = 0, 1, 2, \ldots$) created by $V(z)$ are much further apart than those created by $V(y)$. When the temperature tends to zero, only the ground state of $V(z)$ is usually occupied. In that case $V(z)$ drops out of the calculation of g_{12} apart from the fact that the de Broglie wavelength λ is now given by $(\hbar^2/2m^*)(2\pi/\lambda)^2 = \epsilon_F - \epsilon_{zo}$

where ϵ_F is the Fermi level. When ϵ_F is high enough for electrons to occupy some excited states of $V(z)$ it is only necessary to repeat this calculation for each occupied level ϵ_{zn} and add the results. This argument is valid only when $V(y)$ is strictly independent of z. If the variation of $V(y)$ across the narrow 2D electron gas is significant then full 3D calculations are necessary which would entail a very large increase of computer time.

References

[1] Butcher P N and McInnes J A 1995 *J. Phys.: Condens. Matter* **7** 745
[2] Xu G, Jiang L, Jiang P, Dang L and Xides X 1995 *Phys. Rev.* B **51** 2287
[3] Szafar A and Stone A D 1990 *Phys. Rev. Lett.* **62** 300
[4] Baranger H U and Stone A D 1989 *Phys. Rev.* B **40** 8169
[5] Baranger H U, DiVicenzo D P, Jalabert R A and Stone A D *Phys. Rev.* B **44** 10637
[6] Kirczenow G 1988 *Solid State Commun.* **68** 715
[7] Kirczenow G 1989 *J. Phys.: Condens. Matter* **1** 305
[8] Kirczenow G 1989 *Phys. Rev.* B **39** 10452
[9] Maslov D L, Barnes C and Kirczenow G 1993 *Phys. Rev.* B **48** 2543
[10] Escapa L and Garcia N 1989 *J. Phys.: Condens. Matter* **1** 2125
[11] Garcia N and Escapa L 1989 *Appl. Phys. Lett.* **54** 1418
[12] Tekman E nd Ciraci S 1989 *Phys. Rev.* B **39** 8772
[13] Avishai Y and Band Y B 1989 *Phys. Rev.* B **40** 3429, 12535; *Phys. Rev. Lett.* **62** 2527; 1990 *Phys. Rev.* B **41** 3253; 1991 *Phys. Rev. Lett.* **66** 1761
[14] Li Z-L and Berggren K-L 1992 *Phys. Rev.* B **45** 6652